*Korean J. Chem. Eng.*, **31**(4), 624-629 (2014)
DOI: 10.1007/s11814-013-0272-8

pISSN: 0256-1115
eISSN: 1975-7220

# Characteristics of pellet-type adsorbents prepared from water treatment sludge and their effect on trimethylamine removal

**Junghyun Bae*, Nayoung Park*, Goun Kim*, Choul Ho Lee*, Young-Kwon Park**, and Jong-Ki Jeon*,†**

*Department of Chemical Engineering, Kongju National University, Cheonan 330-717, Korea
**School of Environmental Engineering, University of Seoul, Seoul 130-743, Korea
(*Received 14 April 2013 • accepted 13 December 2013*)

**Abstract**−We optimized the preparation method of pellet-type adsorbents based on alum sludge with the aim of developing a high-performance material for the adsorption of gaseous trimethylamine. Effects of calcination temperature on physical and chemical properties of pellet-type adsorbents were investigated. The porous structure and surface characteristics of the adsorbents were studied using $N_2$ adsorption and desorption isotherms, scanning electron microscope, X-ray diffraction, temperature-programmed desorption of ammonia, and infrared spectroscopy of adsorbed pyridine. The adsorbents obtained from the water treatment sludge are microporous materials with well-developed mesoporosity. The pellet-type adsorbent calcined at 500 °C had the highest percentage of micropore volume and the smallest average pore diameter. The highest adsorption capacity in trimethylamine removal attained over the pellet-type adsorbent calcined at 500 °C can be attributed to the highest number of acid sites as well as the well-developed microporosity.

Keywords: Pellet-type Adsorbent, Water Treatment Sludge, Microporous Material, Acidity, Trimethylamine

## INTRODUCTION

Population growth and industrial development have led to increasing water use, which in turn has spurred the development of water treatment facilities and resulted in increasing amounts of water treatment sludge. The two types of wastes in a water treatment plant, solid and liquid sludge, are usually produced in the precipitation and cleaning processes of water treatment. General water treatment sludge contains 35-50% $SiO_2$, 20-30% $Al_2O_3$, and 15-30% organic matter and water. In 2008, South Korean water treatment plants produced approximately 260,000 tons of water treatment sludge [1]. Moreover, the cost of waste sludge disposal is a major factor in the operational cost of water treatment plants [2].

Water treatment sludge is disposed of through reclamation, ocean dumping, and recycling. The reclamation approach has almost been put to an end due to the difficulties involved in securing landfills. Ocean dumping has the advantage of relatively cheaper disposal costs, but has been prohibited since 2013 [1]. These circumstances have accordingly created an enormous demand for recycling disposal technology. Various sludge utilization methods have been proposed, such as addition to cement, fertilizer production, landfilling, road building materials, incineration to produce energy, production of ceramics, and their use as adsorbents [1,3-5].

Water treatment sludge, however, contains heavy metals and harmful chemicals and thus is difficult to recycle in composts, landfill embankment materials, lightweight aggregate, soil ameliorants, and inorganic fertilizers. Furthermore, drying and incinerating sludge, and fusing and recycling incineration ashes entail excessive energy consumption. Thus there is an urgent need to develop technologies to utilize water treatment sludge as a resource by recycling and putting it to useful purposes [1].

The major components of water treatment sludge are $Al_2O_3$ and $SiO_2$, as well as a variety of clay minerals. The heat treatment turns it into a new crystalline form through decomposition, recombination, and fusion [1]. This approach has attracted the attention of scientists and engineers because the adsorption capacities of sludge derived materials are comparable to those of classic adsorbents such as activated carbons [1,3,5-8]. Considering that water treatment sludge also contains 30% $Al_2O_3$, an inorganic matter, it can also be turned into zeolite to be used in absorbents, catalysts, and ion exchangers [1,5]. Recently, Kang et al. investigated the formation of $AlPO_4$-type porous materials from alum sludge and reported that $AlPO_4$-type porous materials from alum sludge might be applicable in the removal of toxic volatile organic compounds from the air [1].

Trimethylamine (TMA) is a volatile organic compound responsible for strong odor emissions. It is often released from fish-meal manufacturing processes, wastewater treatment, waste disposal landfills, livestock farming, and hog manure. Due to its potentially toxic and likely carcinogenic properties, TMA is considered a strong environmental pollutant [9].

We optimized the preparation method of pellet-type adsorbents based on alum sludge with the aim of developing a high-performance material for the adsorption of gaseous TMA. Using an extruding machine, we developed a process for continuous extrusion production of pellet-type adsorbents composed of alum sludge powder and a binder. Effects of calcination temperature on physical and chemical properties temperature of pellet-type adsorbents were investigated. The porous structure and surface characteristics of the adsorbents were studied using $N_2$ adsorption and desorption isotherms, scanning electron microscope (SEM), X-ray diffraction (XRD), temperature-programmed desorption of ammonia ($NH_3$-TPD), and Fourier transform infrared spectroscopy (FT-IR) of adsorbed pyridine.

†To whom correspondence should be addressed.
E-mail: jkjeon@kongju.ac.kr

## EXPERIMENTAL

### 1. Preparation of the Adsorbents

A powder-type sludge from water treatment sludge (raw sludge) was produced as follows. We put 1 kg of water treatment sludge, 400 g of water, and 100 g of $H_3PO_4$ (85%, Junsei Chemical Co.) in a batch-type reactor, kept it at 110 °C, and promoted a hydration reaction by stirring it for two hours. The resulting solid was filtered with filter cloth, washed with purified water, and dried at 60 °C for 24 hours. The cake-type sludge was then pulverized and turned into powder. This powder was dried at 110 °C for 12 hours.

Powder-type sludge (400 g) was mixed with 250 g of water and 20 g of methyl cellulose as a binder. An extruding machine with a dual screw and a die with 37 cells (the diameter of each cell was 4.5 m) were used. A mixture of powder type sludge, methyl cellulose, and water was injected into the hopper equipped over the extruder to feed the mixture. The extrusion speed was then controlled by maintaining the barrel rotation speed at approximately 40 rpm. The extrudates were cut to a certain size, dried at 110 °C for 24 hours, and calcined at a specified temperature for four hours. The calcination temperature of absorbents was altered in a range of 300-600 °C in order to investigate the effects of calcination temperature on their characteristics and capacity to eliminate trimethylamine. The pellet-type adsorbents prepared from water treatment sludge in this study are denoted 'SA', and the numbers refer to the calcination temperature. As an example, SA500 means the pellet-type adsorbent calcined at 500 °C.

### 2. Characterization of the Adsorbents

The surface area of pellet-type adsorbents for air purification is one of the key properties in evaluating the adsorption performance of air pollutants [10]. The BET surface area of the pellet-type adsorbents was measured with a Belsorp-mini ll apparatus supplied by Bel-Japan. After a sample was dried, 0.3 g was taken. After 5 h of outgassing in a vacuum, nitrogen was supplied as an adsorption gas at the temperature of liquid nitrogen, and nitrogen adsorption-desorption isotherms and the BET surface area were obtained. Micropore volume was evaluated by the t-plot method and the pore size distribution obtained using the Brunauer-Joyner-Halenda (BJH) model.

The compressive strength represents the resistance of the solid to compression, a property of paramount importance for industrial catalysts and adsorbents [11]. The compressive strength was measured as the sample was destroyed by supplying a force onto the sample using an UTM device (H25KS, Hounsfield) at a velocity of 1 mm/min. A thermogravimetric analysis (TGA) was carried out (TGA 2050, TA Instruments) in the presence of air at heating rates of 5 °C/min. A fluorescence X-ray element analyzer (Seico, SEA2220A) was used to measure the amount of metal in the sample. Before these analyses, a sample pre-processor (Milstone/Ethos Touch Control) was used, where 7 ml of nitric acid and 2 ml of hydrochloric acid were added to 0.2 g of the sample, followed by heating at 453 K for 17 min before sample introduction to the ICP-AES instrument. The crystallinity of the samples was investigated with an X-ray diffractometer, a Rigaku Miniflex 600 device using Cu K$\alpha$ radiation energy. A morphological characterization of the samples was done with a scanning electron microscope (FE-SEM, JSM-6335F, Jeol). The sample was dropped onto the surface of the sample holder and then placed under a vacuum at room temperature; all samples were coated with gold prior to being examined.

The acidic property of the sample was analyzed by TPD of chemisorbed ammonia [12,13]. A 0.02 g sample was placed in a quartz tubular reactor and pretreated in a helium flow, heated to 300 °C with 10 °C/min, and kept at 300 °C for 2 h. The samples were cooled to 100 °C and an ammonia pulse was injected. After the physisorbed ammonia was purged with helium, TPD was performed.

The nature of the acid sites was investigated using pyridine as a probe molecule. Pyridine is favored for quantification of Brønsted acid sites and Lewis acid sites separately since its adsorption on Brønsted acid sites and Lewis acid sites gives discrete IR bands [14]. Pyridinium ions formed via protonation of the pyridine molecule react with Brønsted acid sites are most conveniently detected by an IR band at about 1,540 $cm^{-1}$, whereas pyridine is coordinatively adsorbed on a Lewis acid sites and gives rise to a well-resolved band at about 1,450 $cm^{-1}$. Self-supported wafers of the samples were prepared with 3 tons of pressure applied. All the samples were subjected to a vacuum in the sample holder until a pressure of $10^{-3}$ torr was attained, followed by their activation at 300 °C for 1 h. Pyridine vapor was admitted in doses until the catalyst surface was saturated. Pyridine was then desorbed until a pressure of $10^{-3}$ torr was reached to ensure that there was no more physisorbed pyridine on the wafers. IR spectra were recorded using a Spectrum GX (Perkin Elmer) with an MCT detector. The wafers that contained chemisorbed pyridine were subjected to thermal treatment at 100, 150, 200, 250, and 300 °C, and the IR spectra were recorded in situ at those temperatures.

### 3. TMA Adsorption

A custom-designed dynamic test was used to evaluate the performance of adsorbents for TMA adsorption from gas streams. 6 g of pellet-type adsorbent samples (4.5 mm diameter and 8 mm length) was packed into a glass column (length 270 mm, internal diameter 20 mm, bed volume 30 $cm^3$). A gas mixture containing 0.1% (1,000 ppm) of TMA was passed through the column of adsorbent with a flow rate of 50 ml/min. The flow rate was controlled by using a mass flow controller (Brooks). The breakthrough curve of TMA was monitored with an online gas chromatograph (Donam Instruments Co., DS 6200) equipped with FID and a Carbowax amine capillary column (30 m×0.53 mm×1.0 μm film thickness).

## RESULTS AND DISCUSSION

### 1. Characteristics of the Adsorbents

The dry basis compositions of the powder-type sludge are presented in Table 1. The main components of the powder-type sludge are alumina, silica, phosphorus, iron, sulfur, and potassium compounds. The content of the main components in pellet-adsorbents (SA-110) obtained from the sludge is almost the same as that of the powder-type sludge. With an increase of calcination temperature to 500 °C, the content of alumina and silica, which are engaged in the compounds and thus do not vaporize, should slightly increase.

Fig. 1 shows the results of the TGA analysis of the sludge. The weight decreased rapidly at a temperature range of 240-370 °C, but then gradually slowed down and reached almost 35% of the initial weight above 500 °C. At this point all the gaseous and liquid components had been removed, leaving only solid components with large specific surface areas and porous structures, which should be favorable for adsorption.

**Table 1. Results of chemical analysis of powder-type sludge and pellet-type adsorbents**

| Element | Quantity (wt%)[a] | | |
|---|---|---|---|
| | Powder-type sludge | SA110 | SA500 |
| Al | 13.2 | 13.1 | 15.1 |
| Si | 14.4 | 14.6 | 15.3 |
| P | 8.9 | 8.6 | 8.1 |
| Fe | 8.7 | 9.2 | 8.6 |
| S | 3.3 | 3.4 | 2.0 |
| K | 2.4 | 2.5 | 2.4 |

[a]Dry basis quantity measured by fluorescence X-ray element analyzer

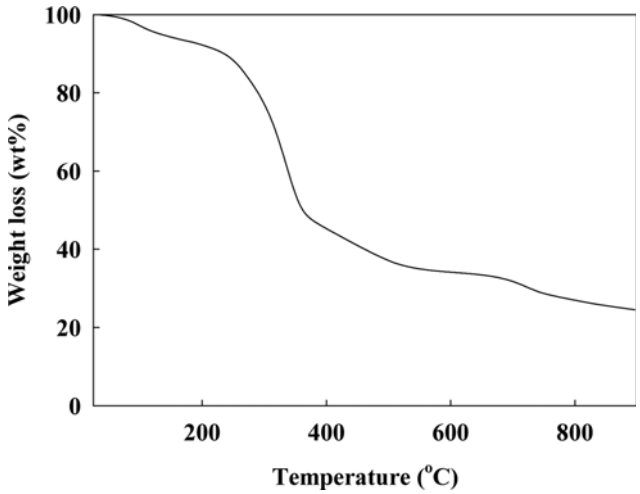


**Fig. 1. TGA curves in nitrogen for the SA110 sample.**

Since the performance of adsorbents in an adsorption process depends on their porosity, parameters related to the porous structure were measured from $N_2$ adsorption. The $N_2$ adsorption and desorption isotherms of the samples are shown in Fig. 2. The lower branch of each isotherm represents measurements obtained by adsorption and the upper branch by desorption. As can be seen from Fig. 2, all five isotherms exhibited a type I with somewhat type IV character nitrogen isotherm in the IUPAC classification, because they had both a sharp rise at low relative pressure and a hysteresis loop [15]. This indicates that they are microporous materials with well-developed mesoporosity [1]. In addition, all of the isotherms showed a type H3 or H4 hysteresis loop in de Boer's classification, which is characteristic of slit-shaped pores [16]. It is clear that the isotherm of SA500 exhibited a type H4 character with a small hysteresis loop, indicating that micropores are the major component of SA500.

The structural parameters calculated from nitrogen isotherms are listed in Table 2, including total BET surface area ($S_{BET}$), single point adsorption total pore volume calculated at $P/P_0$=0.99 ($V_p$), t-plot micropore volume ($V_{micro}$), percentage of micropore volume ($V_{micro}/V_p$), and BJH desorption average pore diameter ($D_p$). It can be seen that the BET surface area of the pellet-type adsorbents was in a range of 157-175 $m^2/g$. The pellet-type adsorbent calcined at 500 °C had the highest percentage of micropore volume and the smallest average pore diameter, which can be confirmed through the pore size distribution of the samples in Fig. 3.

**Table 2. Surface area, pore volume, and pore size of pellet-type adsorbents**

| Sample | $S_{BET}$[a] ($m^2/g$) | $V_p$[b] ($cm^3/g$) | $V_{micro}$[c] ($cm^3/g$) | $V_{micro}/V_p$ (%) | $D_p$[d] (nm) |
|---|---|---|---|---|---|
| SA110 | 82 | 0.19 | 0.03 | 16 | 3.2 |
| SA300 | 158 | 0.51 | 0.01 | 2 | 3.2 |
| SA400 | 175 | 0.29 | 0.08 | 28 | 3.2 |
| SA500 | 157 | 0.17 | 0.11 | 65 | 2.4 |
| SA600 | 161 | 0.37 | 0.04 | 11 | 3.2 |

[a]Calculated in the range of relative pressure ($P/P_0$)=0.05−0.20
[b]Measured at $P/P_0$=0.99
[c]Micropore volume evaluated by the t-plot method
[d]BJH pore sizes obtained from the adsorption branches

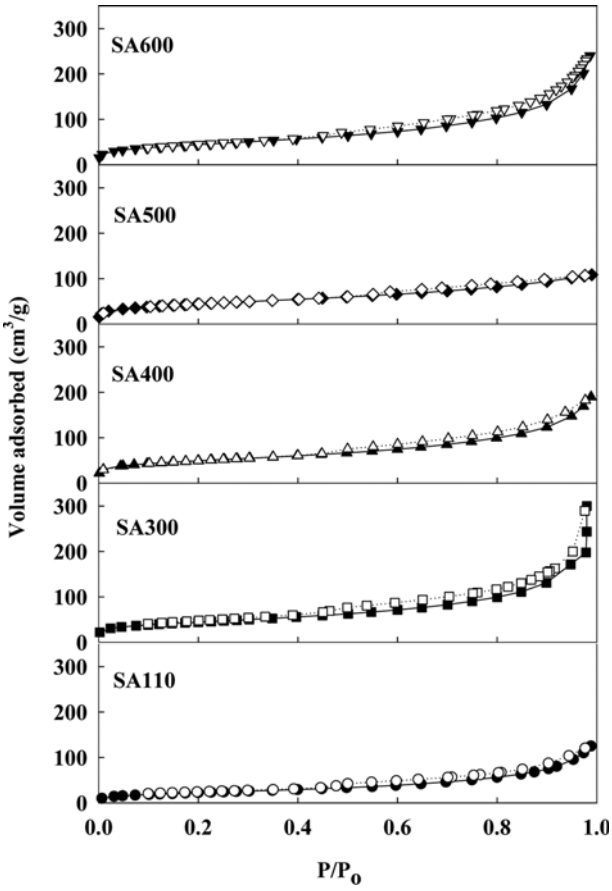


**Fig. 2. Nitrogen adsorption-desorption isotherms of the samples (filled symbol: adsorption, empty symbol: desorption).**

Fig. 4 shows the compressive strengths of the samples. The pellet-type adsorbents calcined at a temperature over 300 °C had weaker compressive strength than that of the pellet-type adsorbent without calcination; this appears to be due to decomposition of methyl cellulose, a binder, during calcination.

Kang et al. analyzed the XRD results of synthesized material to develop the manufacturing process of material synthesized from water treatment alum sludge and treated by phosphoric acid based on a preliminary study [17]. They reported that the material synthesized from a hydrothermal reaction after phosphoric acid treatment

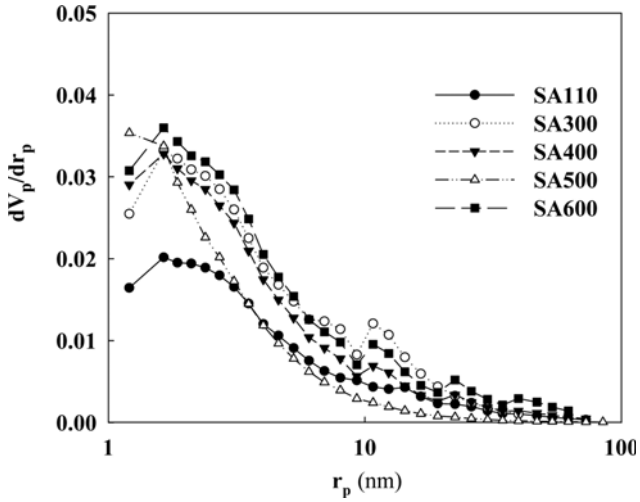


**Fig. 3. Pore size distributions of the samples.**

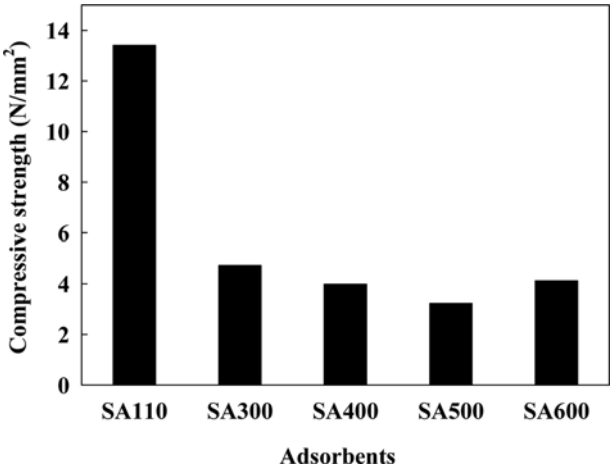


**Fig. 4. Compressive strength of the samples.**

of water treatment alum sludge containing organic matter showed the XRD pattern of $AlPO_4$-type matter. Of the pellet-type absorbents produced in the study, the SA110 sample had $2\theta$ peaks at 25.46° and 26.48° (Fig. 5), which were consistent with the peaks in the JCPDS database of synthetic $AlPO_4$ (JCPDS card No. 34-151) or hydrated $AlPO_4$ (JCPDS card No. 10-0423, 25-0018, 33-32, 33-0033, 34-151) [1]. The sample (SA500) that was calcined at 500 °C showed slightly improved crystallinity but exhibited no major structural changes.

**2. Adsorption of TMA over Pellet-type Adsorbents**

The TMA breakthrough curves measured at room temperature and the adsorption capacity calculated from the breakthrough curve are presented in Fig. 6 and Table 3, respectively. The adsorption capacity of the pellet-type adsorbent increased with increasing calcination temperature from 300 to 500 °C. The adsorption capacity, however, decreased with increasing calcination temperature above 500 °C. The surface areas of the pellet-type adsorbent were not affected significantly with increasing calcination temperature in a range of 300-600 °C, as shown in Table 2. It is noticeable that the pellet-type adsorbent calcined at 500 °C had the highest percentage of micropore volume and the smallest average pore diameter, as shown in Table 2 and Fig. 3. With increasing calcination temperature from 300 to

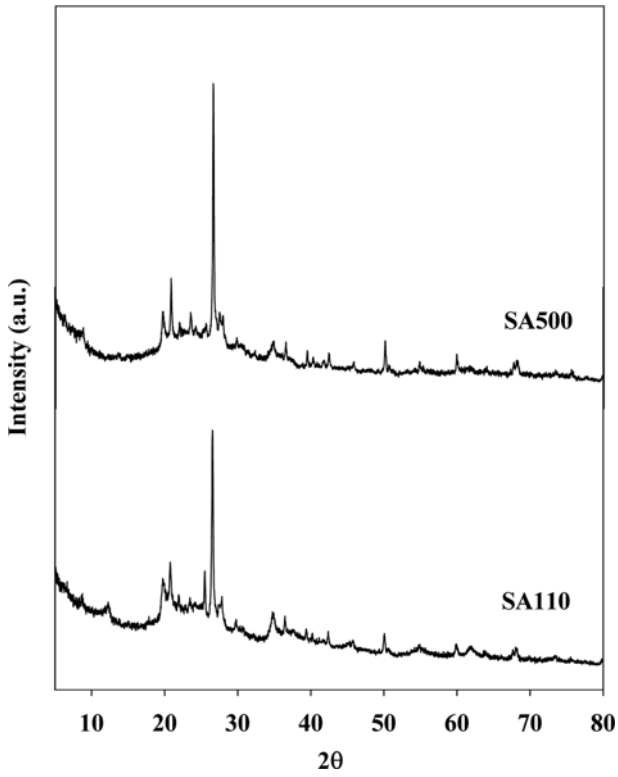


**Fig. 5. XRD patterns of the samples.**

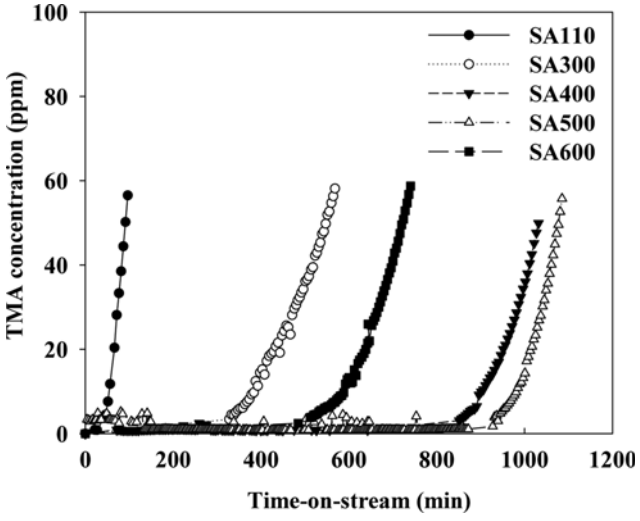


**Fig. 6. TMA breakthrough curves.**

**Table 3. Adsorption capacity of the adsorbents**

| Adsorbents | Adsorption capacity (mg/kg) |
|---|---|
| SA110 | 550 |
| SA300 | 3,567 |
| SA400 | 7,928 |
| SA500 | 8,374 |
| SA600 | 5,295 |

500 °C, the percentage of micropore volume sites increased significantly. Further increase of calcination temperature to 600 °C resulted

in a decrease of the percentage of micropore volume, meanwhile the surface area was almost maintained. Consequently, the order of the samples with respect to the fraction of micropore volume is SA500, SA400, SA600, and SA300, well corresponding to the results of the adsorption capacity. Because larger pore diameter might facilitate the transport of molecules into the pores of the adsorbent, the highest adsorption capacity over the pellet-type adsorbent calcined at 500 °C could be explained by the well-developed microporosity of the adsorbent. In the case of the sample without calcination, SA110, the lowest adsorption capacity among the samples can be ascribed to the smallest surface area.

### 3. Characteristics of Acid Sites over the Pellet-type Adsorbents

$NH_3$-TPD profiles for four samples calcined at different temperatures are given in Fig. 7. The $NH_3$-TPD profile for the sample calcined at 300 °C consisted of a broad peak around 190 °C followed by an overlapping peak at 300 °C. These peaks could be assigned as weak and medium strength acid sites, respectively. The peak intensity of medium strength acid sites over the pellet-type adsorbent increased with increasing calcination temperature from 300 to 500 °C. Further increase of calcination temperature to 600 °C resulted in a decrease of the peak intensity of medium strength acid sites. Consequently, the samples calcined at 500 °C showed the highest number of medium strength acid sites, corresponding closely to the TMA breakthrough results.

Fig. 8 shows the FT-IR spectra of the pyridine adsorbed on the adsorbent calcined at 500 °C, followed by desorption at elevated temperatures from 25 to 300 °C. At lower temperatures below 100 °C,

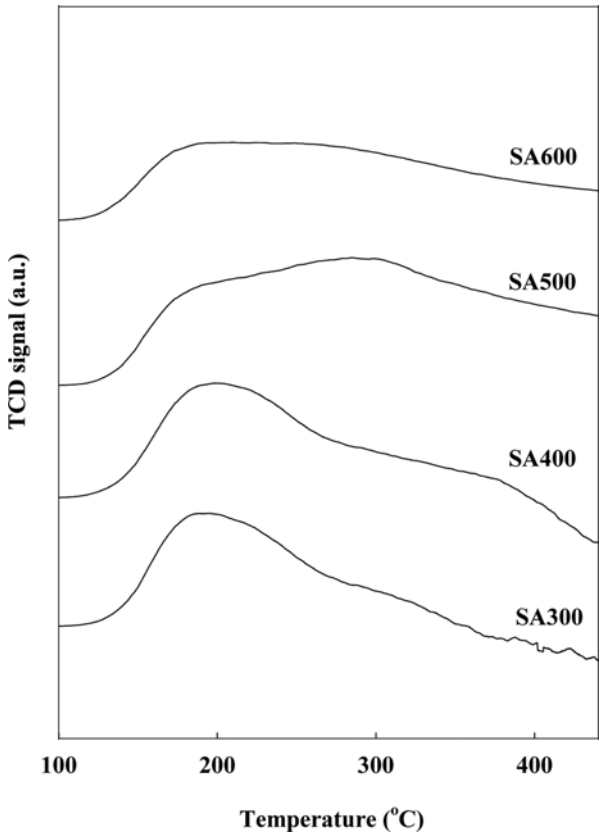


**Fig. 7. Temperature-programmed desorption of ammonia of SA500 and SA600 samples.**

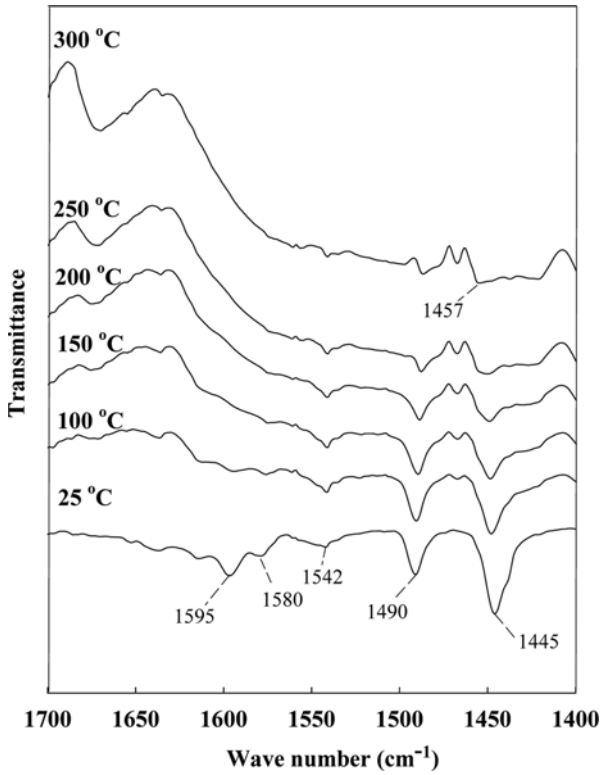


**Fig. 8. FTIR of adsorbed pyridine over the SA500 sample. The sample was desorbed under $10^{-3}$ torr at a range of 25-300 °C.**

five bands at 1,595 $cm^{-1}$, 1,580 $cm^{-1}$, 1,542 $cm^{-1}$, 1,490 $cm^{-1}$, and 1,445 $cm^{-1}$ were detected. An increase in the desorption temperature appears to reduce the intensity of the bands at 1,595 $cm^{-1}$, 1,580 $cm^{-1}$, and 1,445 $cm^{-1}$ more drastically than the intensity of the bands at 1,542 $cm^{-1}$ and 1,490 $cm^{-1}$. At higher temperatures above 200 °C, a band at 1,557 $cm^{-1}$ became evident. Finally, the bands at 1,542 $cm^{-1}$, 1,490 $cm^{-1}$, and 1,457 $cm^{-1}$ were dominant after desorption at 300 °C. It is clear that the bands at 1,542 $cm^{-1}$, 1,490 $cm^{-1}$, and 1,457 $cm^{-1}$ show the presence of higher strength acid sites compared to the bands at 1,595 $cm^{-1}$, 1,580 $cm^{-1}$, and 1,445 $cm^{-1}$. These trends are consistent with those reported in the literature [17-20], and the three bands at 1,542 $cm^{-1}$, 1,490 $cm^{-1}$, and 1,457 $cm^{-1}$ could be assigned to Brønsted acid sites, Brønsted/Lewis acid sites, and Lewis acid sites, respectively [17-20]. It was reported that the bands at 1,595 $cm^{-1}$, 1,580 $cm^{-1}$, and 1,445 $cm^{-1}$ are produced by hydrogen-bonded pyridine with silanol groups. As a result, the adsorbent made from water treatment sludge was found to contain Brønsted acid sites, Lewis acid sites, and H-bond acid sites. Therefore, upon summarizing the results of ammonia TPD and IR spectra of pyridine adsorption, the result that the highest adsorption capacity over the pellet-type adsorbent calcined at 500 °C can be attributed to this condition providing the highest number of acid sites composed of Brönsted acid sites, Lewis acid sites, and H-bond acid sites.

## CONCLUSIONS

The pellet-adsorbents obtained from the water treatment sludge are microporous materials with well-developed mesoporosity. The pellet-type adsorbent calcined around 500 °C had the highest per-

centage of micropore volume and the smallest average pore diameter. The highest adsorption capacity in TMA removal over the pellet-type adsorbent calcined at 500 °C could not be explained by the surface area, but the acidity as well as the pore structure of the adsorbents. Upon summarizing the results of $N_2$ adsorption, $NH_3$-TPD and IR spectra of pyridine adsorption, the result that the highest adsorption capacity over the pellet-type adsorbent calcined at 500 °C can be attributed to this condition providing the highest number of acid sites composed of Brønsted acid sites, Lewis acid sites, and H-bond acid sites as well as the well-developed microporosity.

## ACKNOWLEDGEMENT

This project is supported by Korea Ministry of Environment as "Program for promoting commercialization of promising environmental technologies."

## REFERENCES

1. K. C. Kang, Y. H. Kim, J. M. Kim, C. H. Lee and S. W. Rhee, *Appl. Chem. Eng.*, **22**, 173 (2011).
2. G. R. Xu, Z. C. Yan, Y. C. Wang and N. Wang, *J. Hazard. Mater.*, **161**, 663 (2009).
3. M. Seredych, C. Strydom and T. J. Bandosz, *Waste Manage.*, **28**, 1983 (2008).
4. H. U. Hwang, J. H. Kim and Y. J. Kim, *Original Paper*, **3**, 217 (2009).
5. J. Y. Lee, S. H. Park, J. K. Jeon, K. S. Yoo, S. S. Kim and Y. K. Park, *Korean J. Chem. Eng.*, **28**, 1556 (2011).
6. Z. H. Pan, J. Y. Tian, G. R. Xu, J. J. Li and G. B. Li, *Water Res.*, **45**, 819 (2011).
7. W. Yuan and T. J. Bandosz, *Fuel*, **86**, 2736 (2007).
8. G. R. Xu, W. T. Zhang and G. B. Li, *Water Res.*, **39**, 5175 (2005).
9. Y. Ding, J. Y. Shi, W. X. Wu, J. Yin and Y. X. Chen, *J. Hazard. Mater.*, **143**, 341 (2007).
10. J. W. Lim, Y. H. Choi, H. S. Yoon, Y. K. Park, J. H. Yim and J. K. Jeon, *J. Ind. Eng. Chem.*, **16**, 51 (2010).
11. Y. Li, D. Wu, J. Zhang, L. Chang, D. Wu, Z. Fang and Y. Shi, *Powder Technol*., **113**, 176 (2000).
12. Y. K. Park, S. J. Kim, N. You, J. Cho, S. J. Lee, J. H. Lee and J. K. Jeon, *J. Ind. Eng. Chem*., **17**, 186 (2011).
13. J. K. Jeon and Y. K. Park, *Korean J. Chem. Eng*., **29**, 196 (2012).
14. S. M. Auerbach, K. A. Carrado and P. K. Dutta, *Handbook of zeolite science and technology*, Marcel Dekker, Inc., New York (2003).
15. J. Rouquerol, D. Avnir, C. W. Fairbridge, D. H. Everet, J. H. Haynes, N. Pernicone, J. Ramsay, K. S. Sing and K. K. Unger, *Pure Appl. Chem.*, **66**, 1739 (1994).
16. Z. A. Alothman, *Materials*, **5**, 2874 (2012).
17. B. Chakraborty and B. Viswanathan, *Catal. Today*, **49**, 253 (1999).
18. G. T. Palomino, J. J. C. Pascual, M. R. Delgado, J. B. Parra and C. O. Arean, *Mater. Chem. Phys.*, **85**, 145 (2004).
19. M. I. Zaki, M. A. Hasan, F. A. Al-Sagheer and L. Pasupulety, *Eng. Aspects*, **190**, 261 (2001).
20. M. Yurdakoc, M. Akcay, Y. Tonbul and K. Yurdakoc, *Turk. J. Chem.*, **23**, 319 (1999).